Iranian Journal of Oil & Gas Science and Technology, Vol. 5 (2016), No. 2, pp. 01-20
http://ijogst.put.ac.ir

Application of Well Log Analysis to Assess the Petrophysical Parameters of the Early Eocene Sui Main Limestone (SML) in Kharnhak-1 Well, Middle Indus Basin, Pakistan

Asad Zia[1], Muhammad Awais[2*], Muhammad Ishaq[1], Sardar Hamid[3], Naveed Akhtar[1], and Lawangin Sheikh[2]

[1] National Centre of Excellence in Geology, University of Peshawar, Peshawar-25130, Pakistan
[2] Department of Geology, University of Swabi, Swabi-23561, Pakistan
[3] Department of Geology, University of Peshawar, Peshawar-25120, Pakistan

Received: October 06, 2015; *revised:* December 01, 2015; *accepted:* January 14,2016

Abstract

The petrophysical analysis of the early Eocene Sui Main Limestone (SML) has been conducted in Kharnhak-1 well for the prospect of the hydrocarbon exploration of the Khairpur-Jacobabad High, Middle Indus Basin, Pakistan. The petrophysical analysis of SML is carried out on the basis of well logs including gamma ray, spontaneous potential, resistivity, neutron, and density logs. These analyses lead to interpreting the vertical distribution of porosity and permeability in order to measure the reservoir potential of the SML. The Archie equation was used to assess the petrophysical characteristics. The SML has good porosity and poor permeability with positive correlation coefficient between the two parameters. The average volume of shale is 18%. The log signature of SML shows dominance of carbonates (limestone). The reservoir quality of the SML in Kharnhak-1 well is such that it is 77% water saturated. The porosity (ξ) varies inversely with formation resistivity factor (F) and compressional wave velocity (V_p). However, F and V_p are directly related with each other. Thus, the electric and elastic properties of the carbonate rocks can be influenced by post-depositional alterations, which include porosity enhancement and reduction processes respectively.

Keywords: Petrophysical Analysis, Aui Main Limestone, Well Logs, Archie Equation, Reservoir Quality

1. Introduction

The Eocene carbonate rocks are commercially very significant in the geological history of Pakistan. The central Pakistan was unaffected by the collisional tectonics, being effective in the Northern Pakistan. The Khairpur-Jacobabad High is formed during the Mesozoic when the adjoining areas were rifted apart. They were essentially sub-aqueous islands in an otherwise stable carbonate platform environment (Kadri, 1995). The Eocene rocks are distributed in such a way that it starts from offshore Karachi in the south to the Attock-Cherat Range in the north (Kadri, 1995). The Kharnhak-1 well lies in the Jacobabad Block, Middle Indus Basin (MIB), Pakistan (Figure 1). Geographically, the block is near to the Jacobabad town which is ~375 kilometers north-east-north (NEN) of Karachi, Pakistan.

* Corresponding Author:
Email: awais.geo89@gmail.com

Besides SML, the block consists of Cretaceous Pab and Goru/Sembar sandstones as prospective hydrocarbon horizons (Sheikh, 2003).

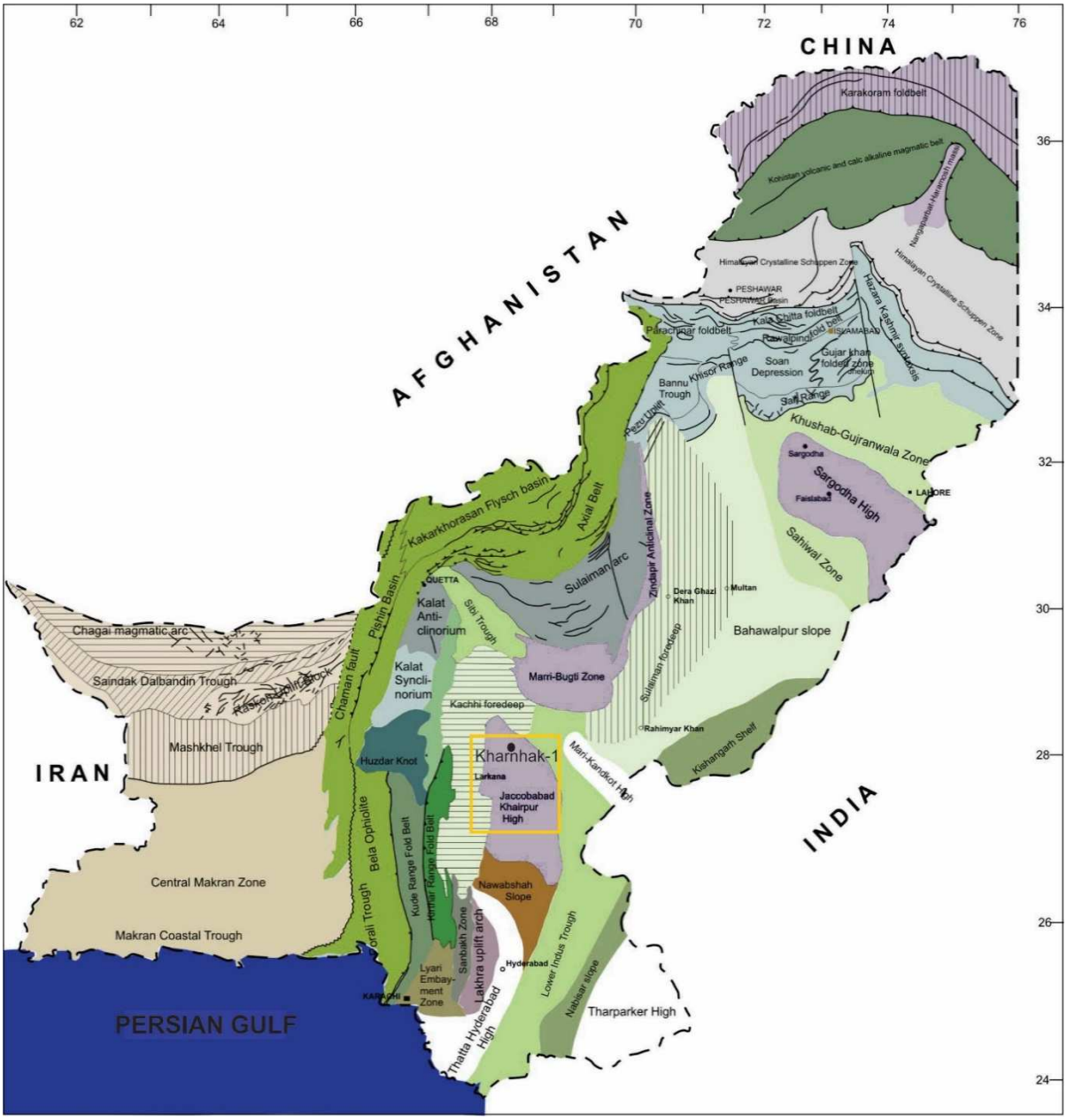

Figure 1
Tectonic map of Pakistan (after Kazmi and Rana, 1982); the inset shows the Khairpur-Jacobabad High having Kharnhak-1 well represented by black dot.

The SML is an ascertained reservoir in the MIB, Pakistan. The name Sui Main Limestone (SML) is given to this prolific gas producing carbonate unit by Pakistan Petroleum Limited (PPL) (Kadri, 1995). More than 20 trillion cubic feet (TCF) of natural gas reserves with minor condensate has been discovered in SML in the 14 gas fields in the region. This amounts to ~50% of the 42 TCF of gas discovered in the last 50 years. It is a big gas reservoir in central Pakistan contributing alone to about 55% of country's annual gas production of 0.924 TCF at an average of 2.53 billion cubic feet (BCF) per day during 2001-2002 (Sheikh, 2003). This research is focused on the petrophysical evaluation to

work out the hydrocarbon potential of SML in Kharnhak-1 well. The lithology of SML is derived from logs. In addition, the relationship between three vital parameters, including formation resistivity factor (F), compressional wave velocity (V_p), and porosity (ξ) involved in formation evaluation is validated. Such inter-relationships help to analyze and draw interpretations about the geological processes based on geophysical logs.

2. Geological setting

The Himalayan orogeny, which has been active since Tertiary, represents collision between the Indian and Eurasian plates (Molnar and Tapponnier, 1977). This collision resulted in the formation of Karakoram thrust zone to the north and Chaman transcurrent fault system to the west ultimately forming MIB. The MIB is situated at latitude of 29º-27º N and longitude of 67º-70º 30/ E in the central portion of Indus basin, Pakistan (Sheikh, 2003). It is surrounded by Sulaiman Fold belt and southern part of Punjab Platform in the north, Indian Shield in the east, Indian Plate marginal zone in the west, and Mari-Kandhkot High in the south. The MIB consists of Mesozoic and Cenozoic rocks. They are encountered in the subsurface during drilling and discerned in outcrop only at the eastern edge of the basin (Iqbal and Shah, 1980; Shah, 1977). Towards the north, the Sargodha High and Pezu uplift separates the MIB from Upper Indus Basin, while Sukkur rift is the division between MIB and southern Indus basin towards the south (Raza et al., 1989).

3. Literature review

In 2005, the Eocene SML is discovered as a gas reservoir due to the discovery through Haseeb well 1. The NNW-SSE oriented anticlinal fold hosts the SML. The limestone having the gas is highly porous with more than 20% matrix and fracture porosity (IPC and GSM, 2007). The SML consists of different facies such as mudstone, wackestone, packstone-grainstone, and dolomitic limestone (Kadri, 1995). The SML overlies Paleocene Ranikot formation and is underlain by Eocene Ghazij shale. The source rock for the gas generation is organic rich Cretaceous shales of Sembar/Goru formations and Ghazij shales are the seal rocks for the SML reservoir (Tainsh et al., 1959; Siddiqui, 2004)). In the northern part of the Khairpur-Jacobabad High, the Ghazij shale is ineffective as a seal above SML due to an increased calcareous content (Siddiqui, 2004). At Sui, this carbonate unit is well developed representing subsurface type-locality (Kadri, 1995). The SML is a closed-system reservoir that is separated in all dimensions by shales or poor reservoir facies and structural barriers (Siddiqui, 2004).

The SML has no outcrop exposure in Pakistan (Kadri, 1995). According to Shah (1977), the measured surface sections by the Geological Survey of Pakistan do not evince the presence of any Eocene limestone between Ghazij shales and the underlying Dungan formation. In subsurface, the SML reservoir-quality facies is restricted within latitude of 29 º-27º N and longitude of 67º-70º E, covering an area of ~50,690 km^2 (Siddiqui, 2004). The SML depositional cycle has a shallow upward trend (Siddiqui, 2004). The SML has good porosity and consists of different pore types such as mouldic, vuggy, intragranular, intercrystalline, and fracture (minor contributor to porosity). In the Haseeb field, more than 20% porosity is recorded in the reservoir zones of SML (IPC and GSM, 2007). In the Sui gas field, the SML is uniform in composition, i.e. limestone with shale intercalations at the top. The porosity varies from 6.7 to 28.4% and the permeability varies from 0.1 to 12.9 millidarcy (md) (Tainsh et al., 1959).

4. Stratigraphy of the Kharnhak-1 well

The general stratigraphy of the MIB starts from Jurassic Chiltan Limestone and reaches Siwaliks of Miocene-Pliocene age, as shown in Figure 2 (Kadri, 1995). Similarly, the stratigraphy of the Kharnhak-1 well starts from the Jurassic Chiltan Limestone. Above the Chiltan Limestone are rocks of Cretaceous age including Sembar formation, Goru formation, Parh Limestone, Mughal Kot formation, and Pab formation. Lying above the Cretaceous sequence are Paleocene Ranikot group and Dungan formation. The Eocene succession is comprised of SML, Sui shale, Sui upper Limestone, Ghazij group, and Kirthar formation. The Eocene rocks are followed unconformably by Siwalik group and alluvium of Miocene-Pliocene and Recent age respectively. The stratigraphic column of the Kharnhak-1 well is shown in Figure 3 (lithology from Shah, 2009).

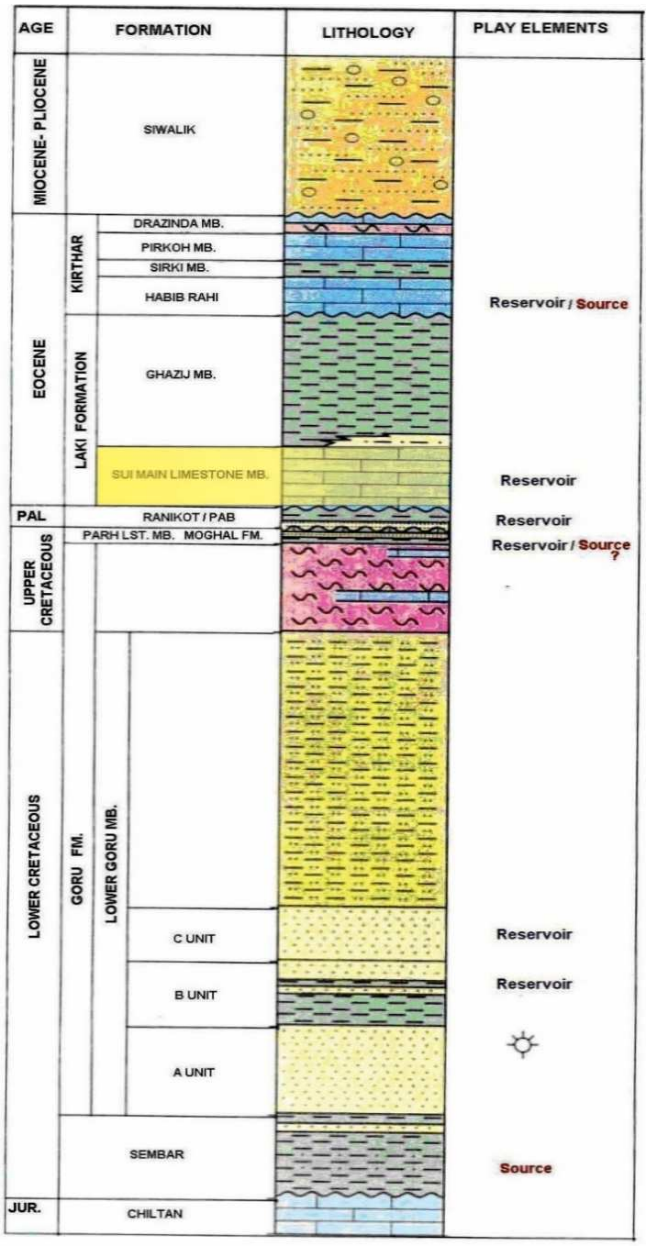

Figure 2
Generalized stratigraphic column of the MIB (after Kadri, 1995).

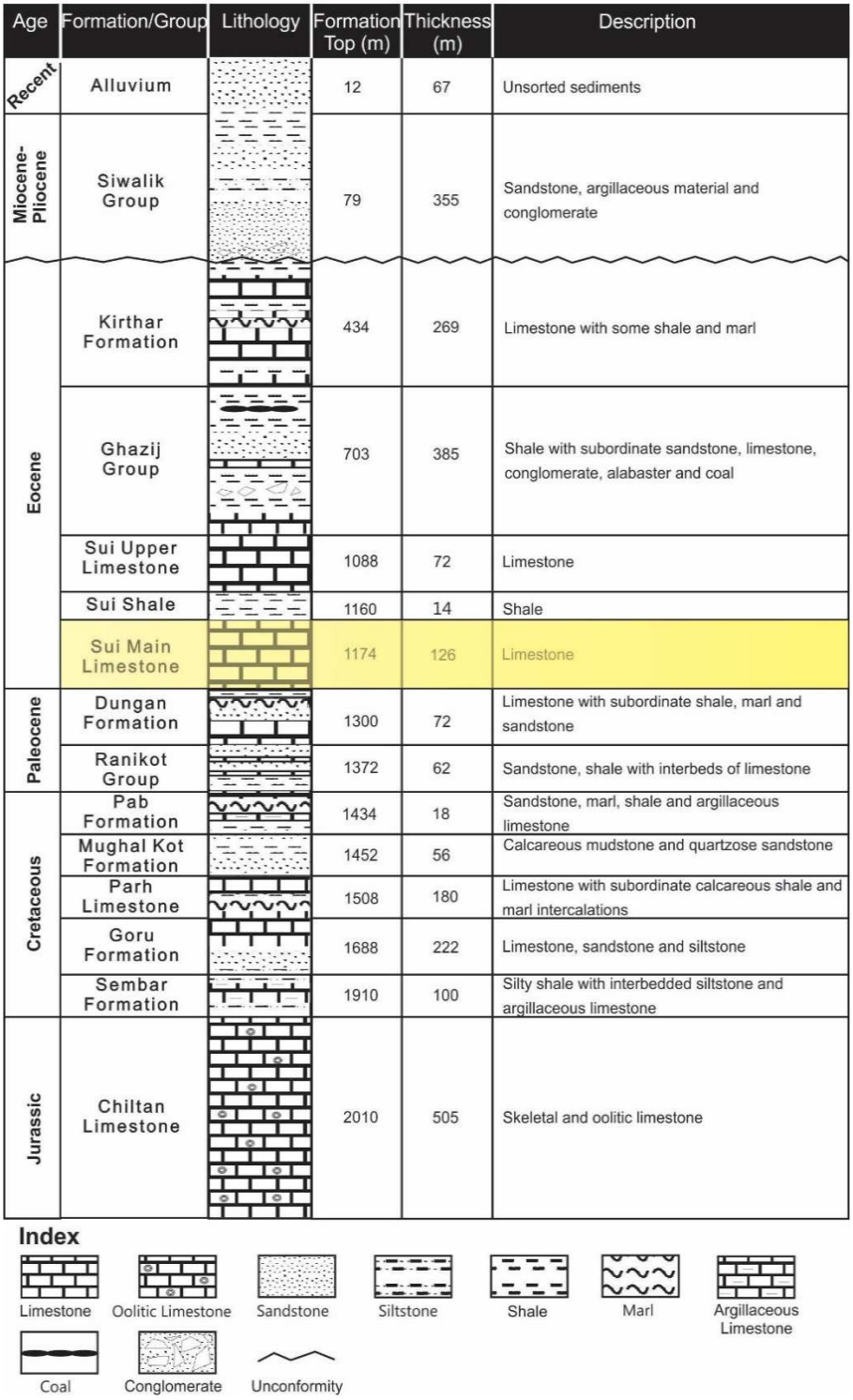

Figure 3
Stratigraphic column of the Kharnhak-1 well (lithology from Shah, 2009).

5. Materials and methods

The petrophysical analyses were performed using well log data. The ξ is determined by using porosity logs, i.e. density, neutron, sonic, and combination of neutron and density logs; permeability (*K*) is calculated from an equation comprised of gamma ray (GR), bulk density (RHOB), deep laterolog

(LLD), acoustic travel time (DT), and neutron porosity (NPHI). The GR log scale is 0-150 API; RHOB ranges from 1.95 to 2.95 g/cc; NPHI ranges from -0.15 to 0.50 (v/v_decimal) porosity unit; spontaneous potential (SP) scale ranges from -70 to -100 mV; the resistivity log scale used is 0.2-2000 ohm.m, and caliper log scale is in the range of 6-16 inches. *F* is defined as the ratio of rock resistivity filled with water (R_o) to the water resistivity (R_w). *F* is inversely related to porosity as mentioned in Equation 1 (Archie, 1942). V_p is the inverse of interval transit time shown in Equation 2 (Peters, 2011). The porosity is the ratio of total vacant spaces to total rock volume shown in Equation 3 (Rider, 1996).

$$F = R_o / R_w = a / \xi^m \quad (1)$$

$$V_p = 10^6 / \Delta t \quad (2)$$

$$\xi = V_p / V_b \quad (3)$$

where, *F* is formation resistivity factor (dimensionless); ξ stands for porosity (%) and *a* represents tortuosity factor; *m* is cementation factor, and *V* denotes compressional wave velocity (ft/s); Δt is interval transit time (μsec/ft); V_p stands for pore volume and V_b represents bulk rock volume.

6. Results and discussion

6.1. Petrophysical evaluation

The petrophysical analyses through wireline logs (GR, RHOB, NPHI, DT, SP, and LLD) for the SML in Kharnhak-1 well were conducted. The analyses were made to calculate the volume of shale (V_{sh}), ξ, *K*, water saturation (S_w), and hydrocarbon saturation (S_{hc}). The GR log is used to measure the amount of shale as a function of depth. The lithologies like shale have high GR reading (>75 API) and clean carbonates have fairly low values, i.e. < 45 API (Rider, 1996). At the depth interval of 1175-1295 m, GR log shows the deflection of varying API as shown in Table 1 (GR maximum used is 95API and minimum is 35API). V_{sh} is calculated from the GR log for the SML interval in Kharnhak-1 well using the following equation (Rider, 1996);

$$V_{sh} = \frac{GR_{log} - GR_{min}}{GR_{max} - GR_{min}} \quad (4)$$

where, V_{sh} is the volume of shale; GR_{log} stands for GR log reading; GR_{max} and GR_{min} represent maximum GR log and minimum GR log respectively.

The density log is a continuous record of formation RHOB. The density porosity (ξ_D) is calculated from the density log using the equation given below (Rider, 1996).

$$\Phi_D = \frac{\rho_{ma} - \rho_b}{\rho_{ma} - \rho_f} \quad (5)$$

where, Φ_D, ρ_b, ρ_{ma}, and ρ_f are density porosity, density from log, matrix density, and fluid density respectively. The lithology is assumed to be pure limestone, so matrix density (ρ_{ma}) is equal to 2.71 g/cc and the fluid density (ρ_f) equals to 1.14 g/cc (Rider, 1996). The density porosity is also calculated by using a Schlumberger standard chart as shown in Figure 4 (Schlumberger, 2009). The NPHI (ξ_N) measures the hydrogen ion in the formation and is read directly from tool (Rider, 1996). The apparent neutron porosity, ξ_N (p.u.), in limestone is calculated from true porosity, ξ (p.u.), for an indicated

matrix (limestone) material by using a chart as shown in Figure 5 (Schlumberger, 2009). The combined neutron-density logs were used to calculate the average neutron-density porosity (Φ_{N-D}) using the given equation (Rider, 1996):

$$\Phi_{N-D} = \frac{\Phi_N + \Phi_D}{2} \tag{6}$$

where, Φ_{N-D} is combined neutron-density porosity and Φ_N represents neutron porosity; Φ_D denotes density porosity. The sonic log is a porosity log (Φ_s) that measures the interval transit time 'delta t' (Δt) of a compressional sound wave traveling through the formation along the axis of borehole in real time and convert it to velocity for lithology, seismic, and geotechnical purposes (Thomas, 1978 and Purdy, 1982). The interval transit time depends upon both lithology and ξ (Rider, 1996).

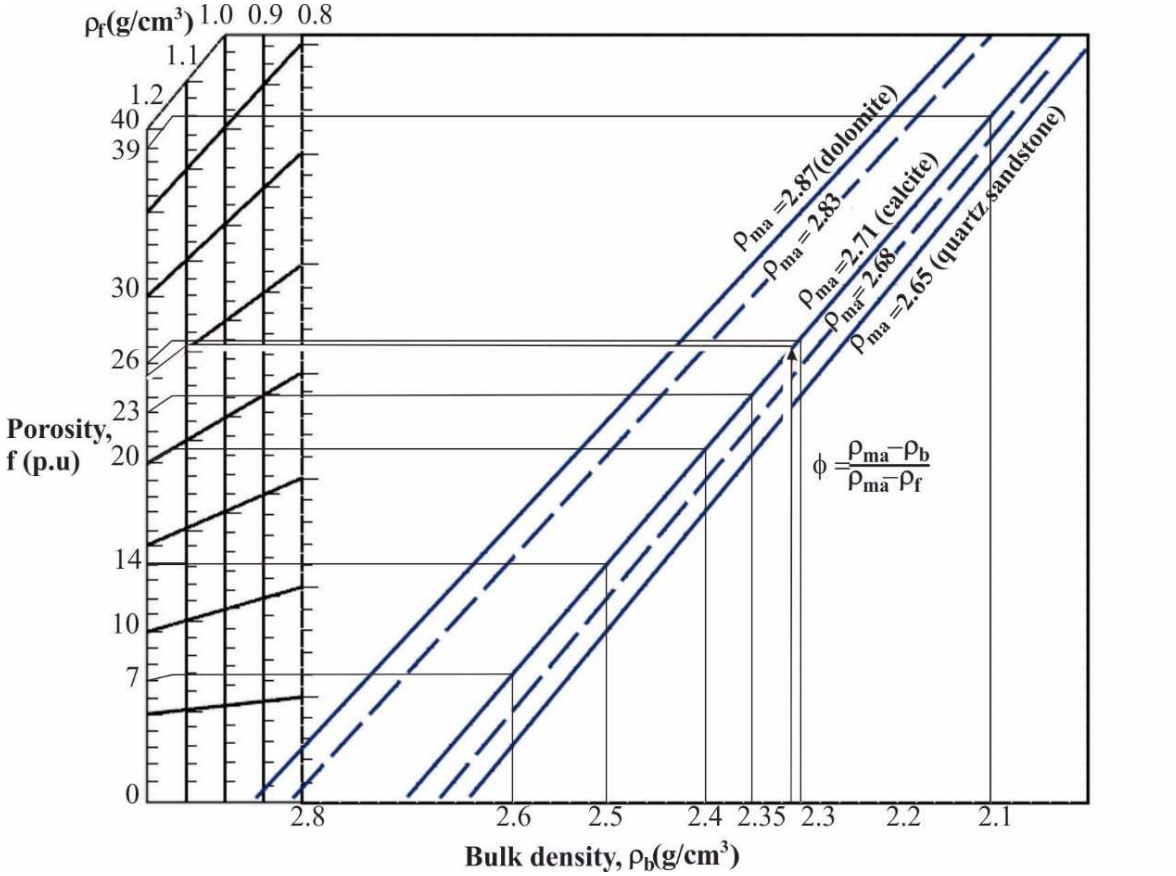

Figure 4
Density porosity determination from bulk density (ρ_b) (Schlumberger, 2009).

The following Wyllie-time average equation is used to calculate sonic porosity with the matrix and fluid interval transit time (Δt_{ma} and Δt_f) of 47.6 µsec/ft and 189 µsec/ft for limestone respectively (Rider, 1996):

$$\Phi_s = \frac{\Delta t_{log} - \Delta t_{ma}}{\Delta t_f - \Delta t_{ma}} \tag{7}$$

where, ξ_s is sonic porosity; Δt_{log} and Δt_{ma} are interval transit time from log and interval transit time of matrix respectively, and Δt_f denotes interval transit time of fluids.

K is calculated using the modified equation of Mohaghegh et al. (1995) for reservoir permeability calculation on the basis of log data reading, with the addition of neutron porosity effect and acoustic travel time to the equation.

$$K = (-38 * GR^{-0.58} + BD^{-0.0044} * LD^{0.28} * DHT^{0.003} * N^{0.4})N^{2.0} \quad (8)$$

where, *K* (mD), GR (API), BD (gr/cc),, and LD (ohm.m), are permeability, gamma ray, bulk density, and deep laterolog respectively; DHT (µ.s/ft) and N (p.u.) stand for acoustic travel time and neutron porosity respectively.

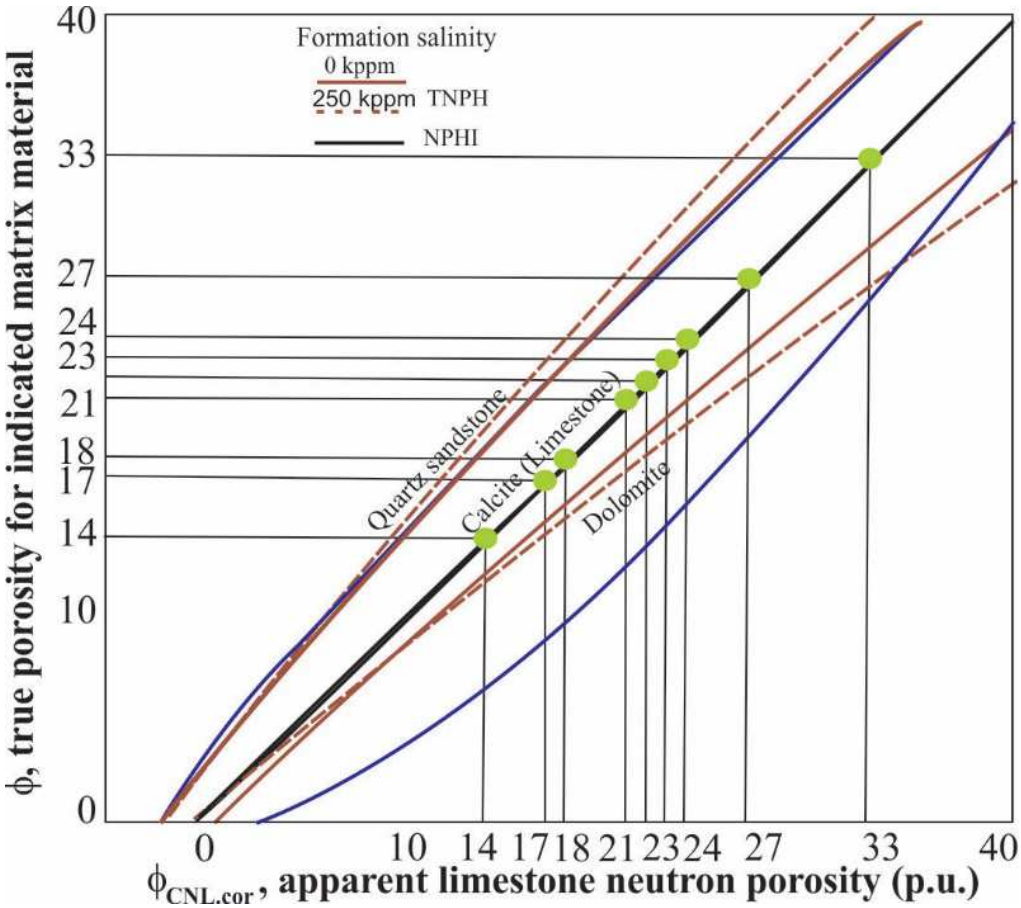

Figure 5
Determination of apparent neutron porosity, ξ_N (p.u.) in limestone (calcite) (Schlumberger, 2009).

The tomography of the porosity and permeability in the Kharnhak-1 well is shown in Figures 6a and b. The porosity displays a positive correlation coefficient (r = 0.55) with permeability, indicating that permeability rises with an increase in porosity. A linear regression equation of $y = 0.014x - 0.2$ is also computed for the porosity and permeability values in the reservoir units of the SML respectively and is utilized to fit a linear regression line to the set of points (Figure 6c). All the petrophysical parameters together with their respective calculated values are given in Table 1.

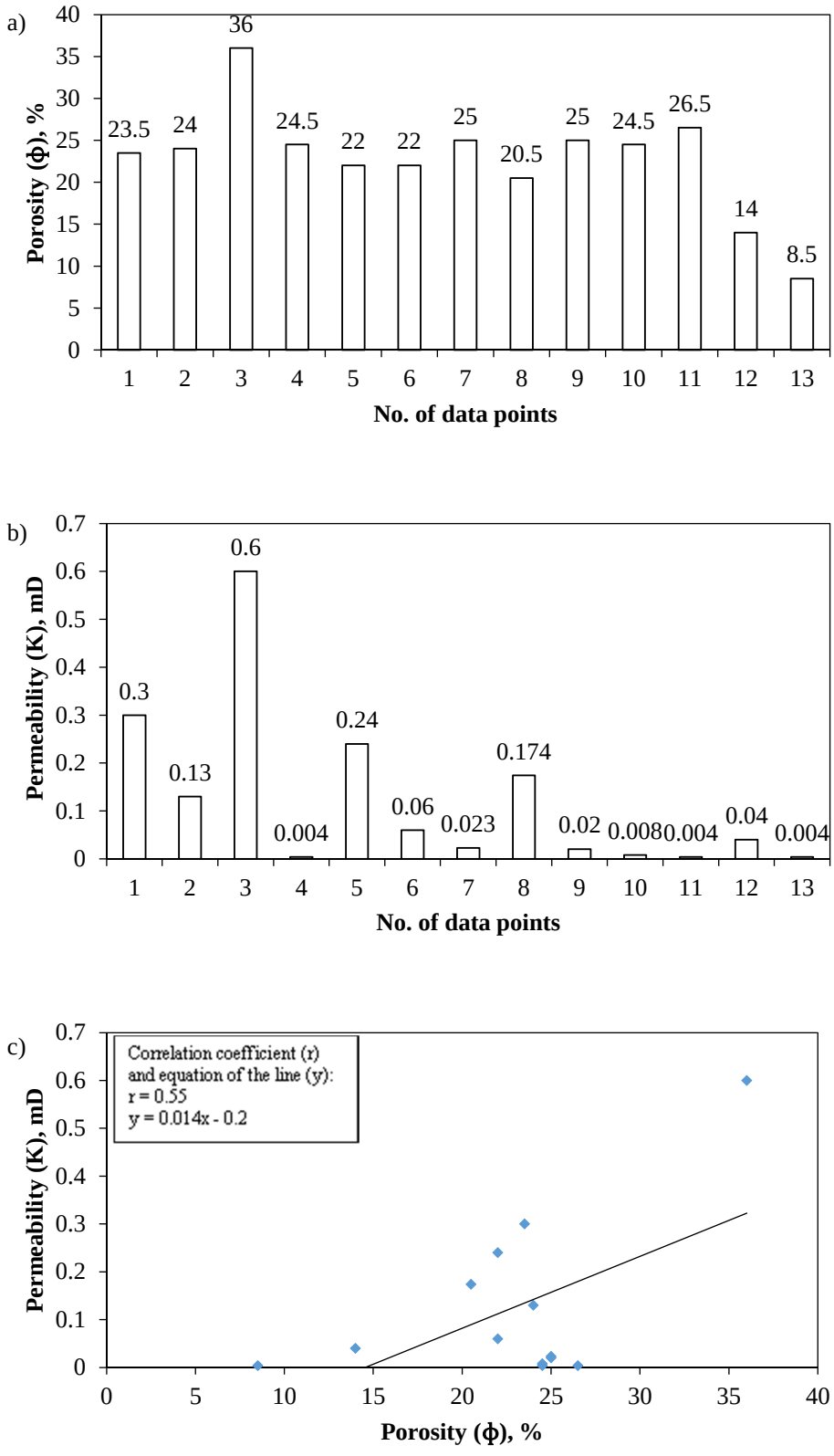

Figure 6

Petrophysical characteristics of the SML in Kharnhak-1 well: (a) and (b) ξ and K tomography of the SML; (c) the relationship between ξ and K of the SML in Kharnhak-1 well.

Table 1:
Values of petrophysical parameters utilized and calculated during petrophysical analysis in Kharnhak-1 well.

Depth (m)	GR_{log} (API)	V_{sh} (%)	ρ_b (g/cc)	ϕ_D (%)	ϕ_N (%)	$\phi_{N\text{-}D}$ (%)	Δt (µsec/ ft)	ϕ_s (%)	R_t (ohm-m)	S_w (%)	S_{hc} (%)	K (mD)
1175	43	13	2.3	26	21	23.5	80	22	1.35	81	19	0.3
1185	43.5	14	2.3	26	22	24	76	20	1.47	76	24	0.13
1195	53	30	2.1	39	33	36	90	29	1.43	51	49	0.6
1205	45	17	2.3	26	23	24.5	116	48	1.85	67	33	0.004
1215	38.5	6	2.4	20	24	22	103	39	1.53	82	18	0.24
1225	43.5	14	2.35	23	21	22	80	22	1.75	76	24	0.06
1235	47.5	21	2.3	26	24	25	79	22	1.69	68	32	0.023
1245	44	15	2.35	23	18	20.5	78	21	1.81	81	19	0.174
1255	43	13	2.3	26	24	25	77	21	1.62	70	30	0.02
1265	47	20	2.3	26	23	24.5	80	22	1.49	74	26	0.008
1275	46.5	19	2.3	26	27	26.5	104	40	1.38	71	29	0.004
1285	47.5	21	2.5	14	14	14	72	17	2.67	97	3	0.04
1295	53	30	2.6	7	17	12	68	14	3.9	94	6	0.004
Average		**18**	**-**	**24**	**22**	**23**	**-**	**26**	**-**	**77**	**23**	**0.124**

The SP log is used to determine the resistivity of formation water (R_w) by applying the following equation (Rider, 1996):

$$SSP = -K\, log \frac{R_{mfe}}{R_{we}} \tag{9}$$

where, K is a constant that depends on formation temperature [K = 65 + (0.24 × formation temperature in ºC)]; R_{mfe} stands for the resistivity of mud filtrate at reservoir temperature, and R_{we} is the equivalent resistivity of water; SSP denotes static SP. Thus, for SML, one may obtain:

$$K = 65 + (0.24 \times 61) = 79.6\,°C \tag{10}$$

The temperature details (surface, maximum bottomhole temperature (BHT), SML top-bottom, and average temperatures are given in Table 2 (Schlumberger, 1974; Wyllie and Rose, 1950). The equivalent mud filtrate resistivity (R_{mfe}) at 61 ºC (average SML temperature) is determined from the chart, as shown in Figure 7, using the value of R_{mf} at the formation temperature (T_f) (Schlumberger, 2009). The R_{mf} at T_f is calculated using the following equation (Schlumberger, 2009):

$$R_{mf}\ at\ T_f\ = R_{mf}\ \frac{(T_1+21.5)}{(T_2+21.5)} \tag{11}$$

where R_{mf} at T_f is the resistivity of mud filtrate at T_f; R_{mf} is the resistivity of mud filtrate at surface temperature; T_2 is the formation temperature and T_1 is the mean surface temperature. The resistivity is in ohm-m and the temperature is given in degrees centigrade. The R_{mf} at T_f is converted to R_{mfe} using a chart (Schlumberger, 2009). The values of R_{mf} at T_f and R_{mfe} in ohm-m are 0.07 and 0.07 respectively (Figure 7).

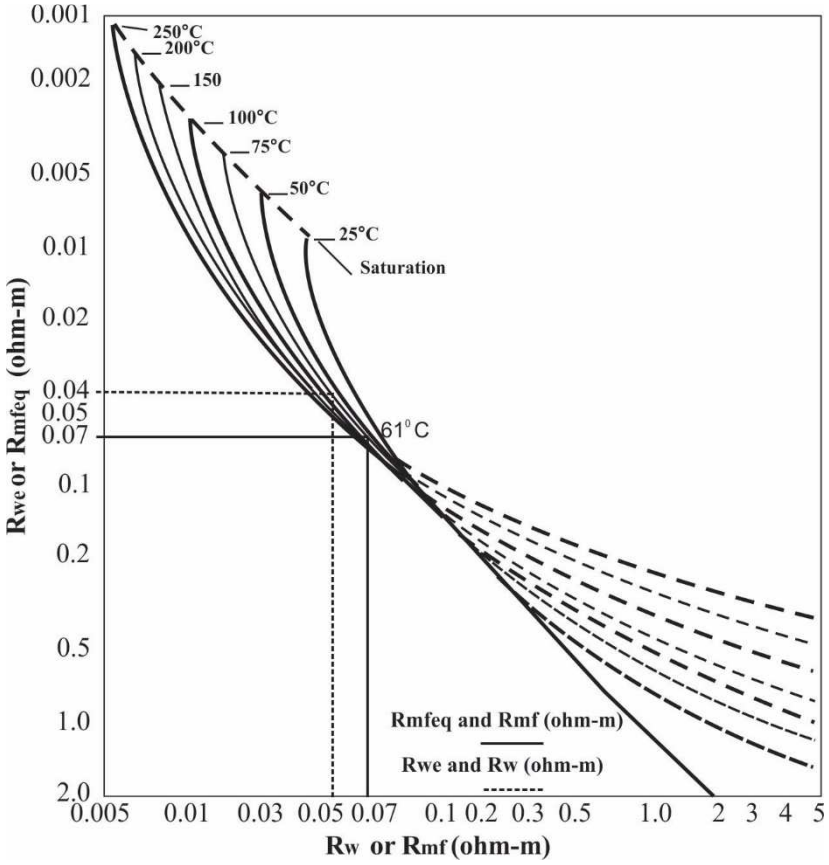

Figure 7
Chart used for converting R_{mf} at T_f to R_{mfe} and R_{we} to R_w (Schlumberger, 2009).

Similarly equivalent water resistivity (R_{we}) can also be calculated from the equation as follows:

$$R_{we} = R_{mfe} \times 10^{\left[\frac{SSP}{61+0.133T_f}\right]} \tag{12}$$

where, T_f is formation temperature in degrees Fahrenheit.

The R_{we} value is converted to R_w at T_f using a chart as shown in Figure 7 (Schlumberger, 2009). The values of R_{we} and R_w are 0.04 and 0.05 respectively (Figure 7). The S_w is calculated through Archie equation as follows (Rider, 1996):

$$S_w = \left[\left(\frac{a}{\phi^m}\right)\left(\frac{R_w}{R_t}\right)\right]^{1/n} \tag{13}$$

where, S_w is water saturation and ξ is porosity; R_w and R_t represent formation water resistivity and true resistivity respectively as read from the deep resistivity log; *a* stands for tortuosity factor (taken as 1), and *m* is cementation factor (taken as 2); n is saturation exponent (taken as 2). *m* values vary from 1.8-3.0 for compacted limestones (Salem and Chilingarian, 1999b). However, Tabibi and Emadi (2003) mentioned that the most applicable values of *m* for carbonate ranges from 1.8 to 2.0. The value of *a* varies from 0.91 to 1.05 and the value of *n* ranges from 2.40 to 4.24 (Elias and Steagall, 1996). S_{hc} is calculated by the given equation (Rider, 1996):

$$S_{hc} = 1 - S_w \quad (14)$$

Table 2
Estimated formation (SML) temperature in Kharnhak-1 well.

Well Name	Surface (ºC)	Maximum BHT (ºC)	Top (ºC)	Bottom (ºC)	Average SML Temperature (ºC)
Kharnhak-1	35	89	59.5	62.3	61

Cut-offs

The cut-offs used for petrophysical interpretation are as follows: V_{sh} cut-off is 30%; ξ cut-off is 15% and S_w cut-off is 60%. The gross, net, net reservoir, and net pay thickness is 126 m, 110 m, 100 m, and 10 m respectively (Figure 8). The net pay has ξ and S_w of 36% and 51% respectively. The net to gross ratio (N/G) is 0.8 representing the presence of clean lithology (limestone).

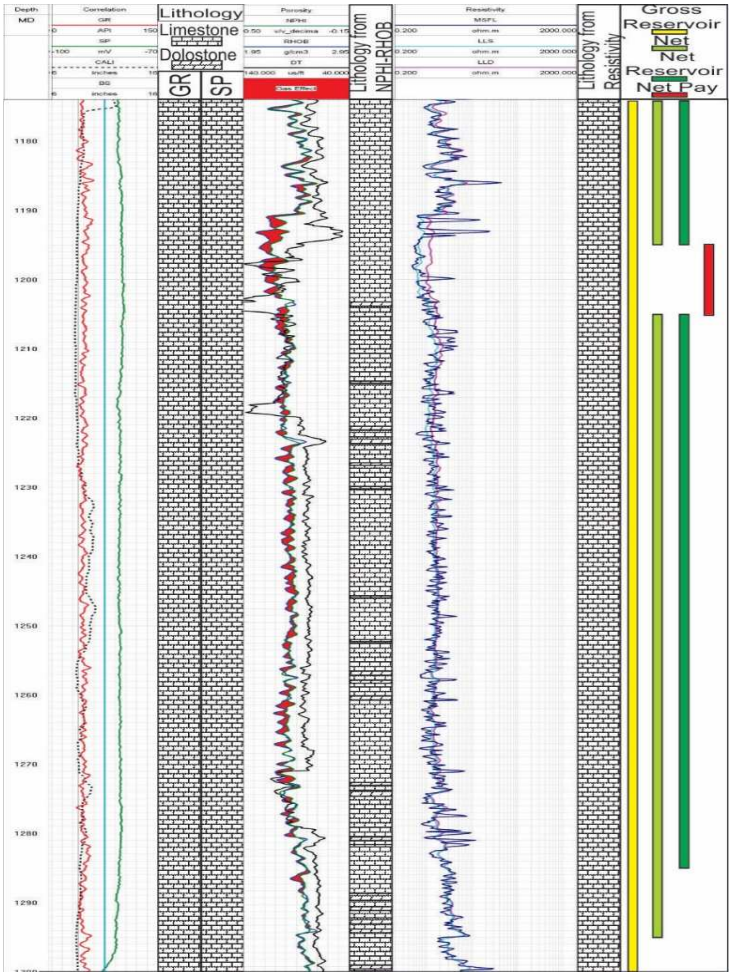

Figure 8
Log signature of SML derived using conventional open hole logs.

The quantitative interpretation is conducted using empirical formulae as given above. In Kharnhak-1 well, SML carbonates have good porosity and poor permeability with higher water saturation (77%). The SML has sufficient porosity to hold hydrocarbons. However, the hydrocarbon saturation is less

(23%) due to ineffective cap rock according to Siddiqui (2004). Therefore, the Kharnhak-1 well is not developed due to insufficient hydrocarbons at SML interval.

6.2. Log Signature of SML

The log signature of SML is derived using conventional open hole logs. This target is achieved by using GR, SP, neutron-density combo, and resistivity logs. In case of GR log, the interpretation is carried out following the work of Adeoye et al. (2013). The GR scale ranges from 0-150 API. A line is drawn at 75 API, above which are the shale intervals and below which are non-shale intervals. In case of SML, the GR log is below 75 API. According to Lucia (2007), the neutron-density combination log is usually utilized to identify limestone and dolostone. The neutron-density logs overlap for limestone, while, for dolostone, there is some gap with a high neutron value to the left relative to the density provided GR curve, which is below shale baseline (Lucia, 2007). Similar technique (combined neutron-density logs) is also used by Hakimi et al. (2015) to interpret the lithology of Sharyoof-1, Sharyoof-2, and Sharyoof-4 wells in Sharyoof oilfield, Masila Basin, Eastern Yemen. In SML, neutron-density combo log signature implies the dominant presence of limestone and minor dolomite. The negative values of SP correspond to the presence of carbonates (limestone). The low resistivity denotes limestone with a high porosity (Figure 8).

Besides Kharnhak-1, there are also two exploratory wells, i.e. Yasin well # 1 and Haseeb well # 1, in Jacobabad block. The distance between Kharnhak-1 and Yasin well # 1 is about 8.5 km, while the distance between Yasin well # 1 and Haseeb well # 1 is about 21 km. The SML of Yasin well # 1 consists of limestone, marl, and shale (Hycarbex Inc., 2008), whereas, in Haseeb well # 1, the SML is composed of limestone (slightly dolomitic), marl, and shale. The thickness of SML in Kharnhak-1, Yasin well # 1, and Haseeb well # 1 is 126 m, 200 m, and 244 m respectively (Figure 9).

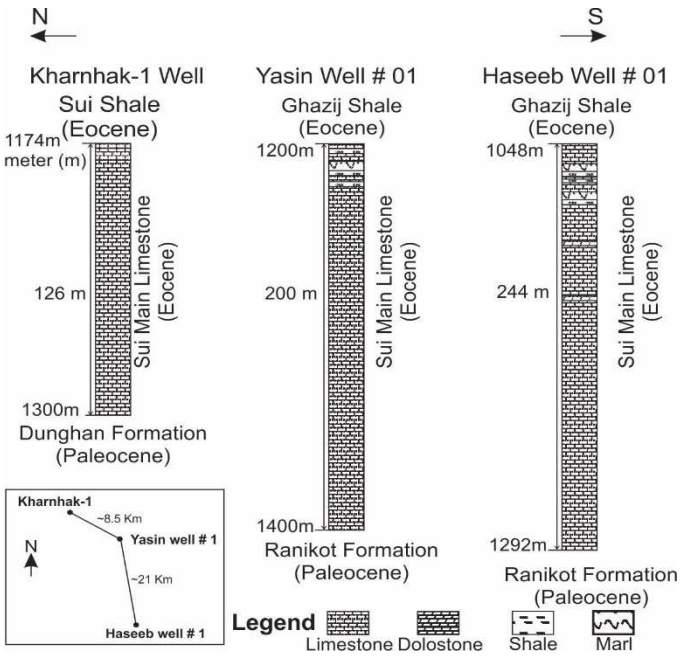

Figure 9
Correlation of SML lithology among Kharnhak-1, Yasin well # 1, and Haseeb well # 1 (Yasin well # 1 and Haseeb well # 1 lithology is taken from IPC and GSM, 2007; Hycarbex Inc., 2008).

Pore types from Sonic Log Response

In carbonates, the pore spaces can be determined by sonic logs. The quantitative porosity analysis can be done in petrographic studies; however, the qualitative studies can be conducted from the sonic log response. Such studies are based on the comparison of the observed response and on the one predicted by the Wyllie equation as shown in Equation 4. As a result, three basic qualitative interpretations can be made: (1) microporous rocks, such as mudstone, plot above the Wyllie line; (2) rocks having intergranular and intercrystalline porosity (sucrosic dolomites) plot on or near the Wyllie line; and (3) rocks with vuggy porosity plot below the Wyllie line (Sadeq and Yusoff, 2015). Sadeq and Yusoff (2015) used the sonic and core porosity cross-plot to infer about the porosity types in carbonates in Bai Hassan oil field, Northern Iraq (Figure 10). However, in this study, the sonic and combined neutron-density crossplot is constructed evincing the presence of micropores, intercrystalline, and vuggy porosity in SML carbonates (Figure 10).

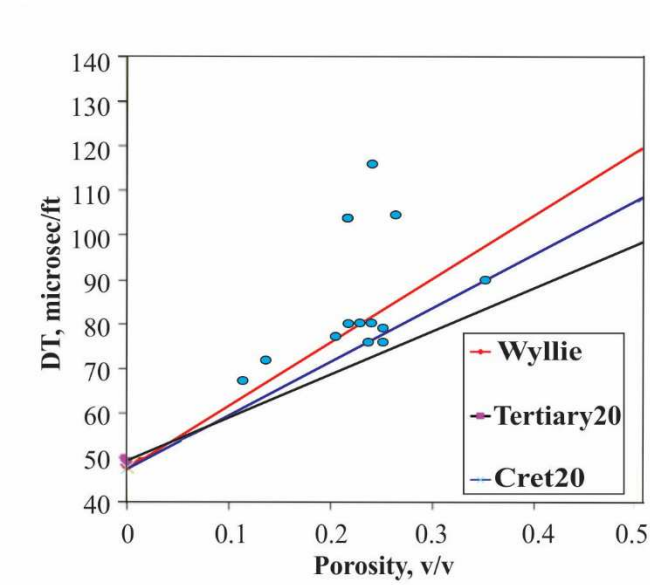

Figure 10
Interpretation of porosity type using sonic versus combined neutron-density porosity (modified from Bai Hassan, sonic versus core porosity of Sadeq and Yusoff, 2015).

Following Hakimi et al. (2015), the pore types within the SML carbonates are interpreted to be dominantly secondary porosity using the cross-plot of the combined neutron-density porosity and sonic porosity (Figure 11). This is also confirmed by the petrographic studies indicating the presence of mouldic, vuggy, and fracture porosity (IPC and GSM, 2007). The qualitative interpretation describes that the SML is predominantly carbonate (limestone) sequence at Kharnhak-1. Similarly, there is secondary porosity as derived from conventional open hole logs.

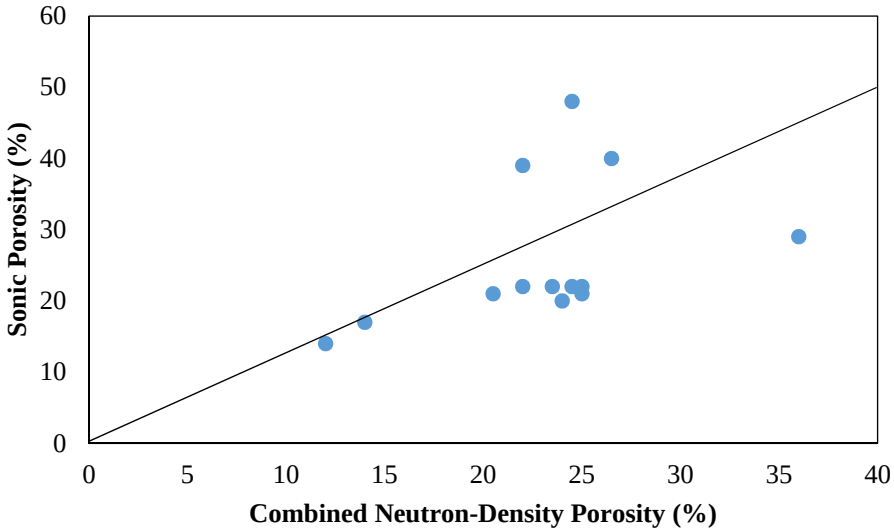

Figure 11
Porosity type identification using the crossplot of combined neutron-density porosity and sonic porosity in SML carbonates (adapted from Hakimi et al., 2015).

7. Relationships between F, V_p, and ξ for the SML

There are three significant parameters in formation evaluation including F, V_p, and ξ. F and V_p are very important parameters in order to work out the electric and elastic behavior of porous media. This leads to interpret the type of fluids present in the pore spaces. F and V_p are controlled by pore and matrix nature, saturation, salinity, water viscosity, formation and pore water resistivity, clay content, cation exchange capacity, bulk density (grains and fluids), fluids type in pores, and different elastic moduli such as pore, fluid, and grain compressibility. Both parameters (F and V_p) are affected by changes in ξ, pressure, and temperature (Salem, 2001).

In this research work, the relationships between F, V_p, and ξ are determined for the SML by utilizing various wireline logs in the Kharnhak-1 well at sampling depth intervals (ΔZ) of 10.0 m. The ξ is calculated from combined neutron-density log and F is determined as a ratio of deep laterolog and water resistivity. The V_p is derived using sonic logs. Table 3 lists the calculated values of the three parameters (F, V_p, and ξ) with a ΔZ of 10.0 m. The relationships that link F, V_p, and ξ are shown in Figures 12a-c. The values of correlation coefficient (r) and the equation of the straight line (y) are given in the mentioned figures. The relationship between these parameters (F, V_p, and ξ) is established by using 13 readings of the reservoir units of the SML for Kharnhak-1 well.

The ξ and F are plotted for the Kharnhak-1 in the reservoir intervals within depth ranging from 1175 to 1295 m. The cross-plot indicates that there is an inverse relationship between the ξ and F. r is -0.78 and $y = 80 - 1.93x$ is computed for the relationship between ξ and F (Figure 12a). V_p is also inversely related to ξ having an r value of -0.53 (Figure 12b; $y = 4998 - 58x$). F and V_p are directly proportional to each other with an r value equal to 0.53 (Figure 12c; $y = 20x + 2922$). An increase in ξ results in a decrease in F and V_p. In contrast, an increase in F consequently enhances V_p.

Table 3
F (dimensionless), V_p (in m/s), and ξ (%) for the SML of Kharnhak-1 well (1174-1300m) at a ΔZ of 10.0 m.

Kharnhak-1			
Sui Main Limestone (1174-1300 m; 126 m)			
***Z* (m)**	***F***	**V_p (m/s)**	**$\phi_{N\text{-}D}$ (%)**
1175	27	3810.976	23.5
1185	29.4	4011.553	24
1195	28.6	3387.534	36
1205	37	2628.259	24.5
1215	30.6	2959.981	22
1225	35	3810.976	22
1235	33.8	3859.216	25
1245	36.2	3908.693	20.5
1255	32.4	3959.455	25
1265	29.8	3810.976	24.5
1275	27.6	2931.52	26.5
1285	53.4	4234.417	14
1295	78	4483.501	12

ξ decreases relatively regularly with depth, while *F* increases with depth; these trends are common irrespective of sediment composition and geographic locality (O'Brien, 1990). The clay content can affect *F* and V_p. The increase in ξ can be due to the presence of shale (clay) and in turn a decrease in *F* and V_p occurs. Within a reservoir rock, shale can be of three types, namely such as structural shale, laminar shale and dispersed shale (Tiab and Donaldson, 2004). In structural shale, ξ is preserved, while the laminar and dispersed shale affects ξ values (Tiab and Donaldson, 2004). Therefore, an increase in shale content implies a decrease in *F* and V_p. In Kharnhak-1 well, the SML dominantly consists of carbonates with a V_{sh} of 18%. There is the presence of argillaceous (clay) and dolomitic lithologies at the interval of SML in Haseeb-1 well (IPC and GSM, 2007). In Yasin well # 1, there is also marl (argillaceous limestone), and shale ultimately raises ξ values but diminishes *F* and V_p (Hycarbex Inc., 2008).

Similarly, in carbonates the ξ variation in relationship to a change in *F* and V_p are related to diagenesis. The diagenetic processes influencing ξ include cementation, neomorphism, dissolution, dolomitization, and fracturing (mechanical compaction) (Flügel, 2010). The cementation and neomorphism can reduce ξ, while dissolution, dolomitization, and fracturing are the main causes of ξ generation and enhancement in carbonates. According to IPC and GSM (2007) mouldic, vuggy, intragranular, intercrystalline, and fracture porosities are noted. This demonstrates that SML

carbonates are modified by diagenetic processes. Hence such diagenetic processes are responsible for the relationship between ξ, *F*, and V_p.

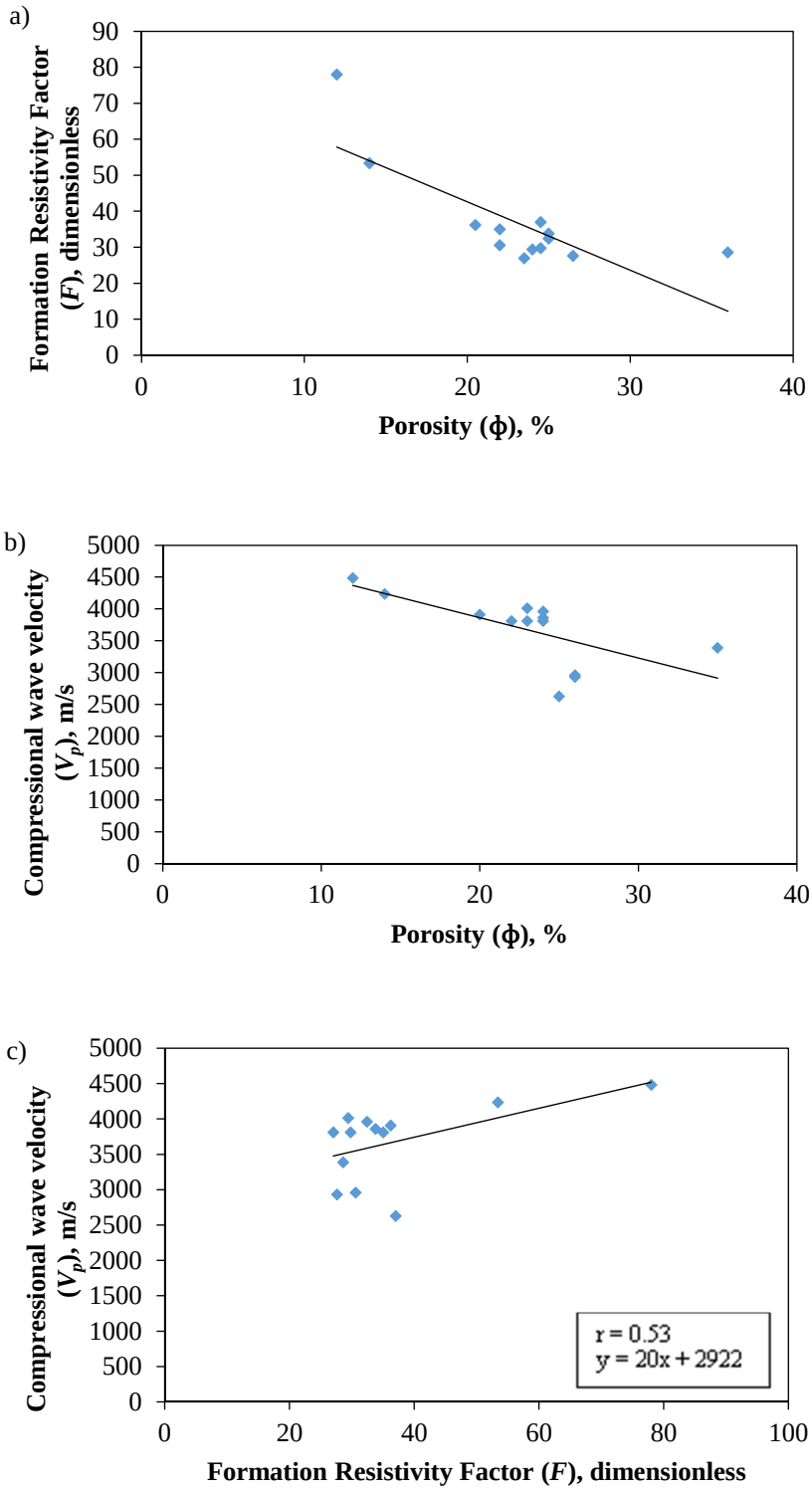

Figure 12
(a) *F* (dimensionless) versus ξ (%); (b) *Vp* (m/s) versus ξ (%); and (c) *Vp* (m/s) versus *F* (dimensionless); 13 readings representing SML of Kharnhak-1 at a *ΔZ* of 10.0 m.

The cemented carbonates will have high F and V_p in combination with the inverse correlation with ξ as compared to non-cemented carbonates. Similarly, ξ enhancement processes like dissolution, dolomitization, diagenetic fractures (open) cause a decrease in F and V_p within the carbonates. The carbonates have high depositional ξ, but as diagenesis begins, it starts diminishing the ξ by early compaction, and later on cement occupies the pore spaces. This results in an increase in F and V_p with reducing ξ. The tectonically fractured carbonates will have low F and V_p as compared to undeformed carbonates provided that the fractures are open. In other words, open fractures raises ξ, while sealed fractures reduces ξ by increasing F and V_p. Hence the elastic and electric character of the carbonate rocks is controlled by ξ enhancement and reducing processes.

8. Conclusions

The reservoir properties of the Eocene SML are evaluated in Kharnhak-1 well located in the Khairpur-Jacobabad High in the MIB, Pakistan. The average V_{sh} is estimated to be 18%. The calculated average ξ_D, ξ_N, $\xi_{N\text{-}D}$, ξ_s, and K are 24%, 22%, 23%, 26%, and 0.124 mD respectively. The ξ shows a positive correlation coefficient (r = 0.55) with K. The higher values of porosities imply higher secondary porosity in carbonates of the SML. In Kharnhak-1, the SML is water-wet with an S_w value of 77.0%, reflecting that SML do not hold hydrocarbon in commercial quantity, and thus should not be developed. The net reservoir and net pay thickness is 100 m and 10 m respectively based on V_{sh}, ξ, and S_w cutoff used. The log signature of SML derived from GR, SP, neutron-density combo, and resistivity logs shows that it is predominantly composed of carbonate (limestone) sequence. The inverse relationship of ξ with F and V_p and the direct relation between the latter two parameters are evidenced in this study. These relationships lead to the interpretation that the electric and elastic characteristics of the carbonate rocks depend upon type of shale, diagenesis, and tectonic processes. It is suggested that an integrated approach should be employed to determine these petrophysical parameters, whereby the results obtained from well logs, core data, and seismic attributes are correlated to get far more vital results.

Acknowledgments

The authors are thankful to the Land Mark Resources (LMKR) and Directorate General of Petroleum Concession of Pakistan, who provided the well data for this research.

Nomenclature

SML	: Sui Main Limestone
MIB	: Middle Indus Basin
PPL	: Pakistan Petroleum Limited
TCF	: Trillion cubic feet
BCF	: Billion cubic feet
ξ	: Porosity (%)
F	: Formation resistivity factor (dimensionless)
V_p	: Compressional wave velocity (ft/s)
K	: Permeability (millidarcy)
GR	: Gamma ray (API)
SP	: Spontaneous potential (mV)
SSP	: Static spontaneous potential (mV)
RHOB	: Bulk density (g/cc)

LLD	: Deep laterolog (ohm.m)
DT	: Acoustic travel time (microseconds/ft)
NPHI	: Neutron porosity (p.u.)
API	: American Petroleum Institute
a	: Tortuosity factor
m	: Cementation factor
n	: Saturation exponent
ρ	: Density (g/cc)
r	: Correlation coefficient
y	: Linear regression equation
p.u.	: Porosity unit
N/G	: Net to gross ratio
BHT	: Bottom hole temperature (°C)

References

Adeoye, O. T. and Ofomola, M. O., Reservoir Characterization of Merit Field (South Western, Niger Delta) from Well Log Petrophysical Analysis and Sequence Stratigraphy, The Pacific Journal of Science and Technology, Vol. 14, No. 1, p. 571-585, 2013.

Archie, G. E., The Electrical Resistivity Log as an Aid in Determining Some Reservoir Characteristics, Transaction of American Institute of Mining, Metallurgical and Petroleum Engineers (AIME), Vol. 146, p. 54-62, 1942.

Elias, V. L. G. and Steagall, D. E., The Impact of the Values of Cementation Factor and Saturation Exponent in the Calculation of Water Saturation for Macaé Formation, Campos Basin, SCA Conference Paper Number 9611, 1996.

Flügel, E., Microfacies of Carbonate Rocks-analysis, Interpretation and Application, 2nd Edition, Springer-verlag, Berlin, Heidelberg, 2010.

Hakimi, M. H. Al-Sufi, S. A., Al-Hamadi, S., and Al-Sharabi, S. A., Petrophysical Analysis of Early Cretaceous Saar Carbonates from Sharyoof Oilfield in the Masila Basin, Eastern Yemen, and their Impact on Reservoir Properties and Quality, Arabian Journal of Geosciences, Vol. 8, No. 12, p. 11307-11319, 2015.

Hycarbex Inc., Exploratory well: Yasin well # 1, Yasin Structure Technical Profile, 2008.

Integrated Petroleum Consultants-IPC (PVT) Limited and GSM, Inc. Texas, USA, Volumetric Reserve Evaluation and Third Party Certification of Haseeb Gas Field Yasin Block (2768-7), Sindh Province-Pakistan for Hycarbex-American Energy Inc., Islamabad, Pakistan, 2007.

Iqbal, M. W. A. and Shah, S. M. I., A Guide to the Stratigraphy of Pakistan, Geological Survey of Pakistan Records, Geological Survey of Pakistan, Quetta, Vol. 53, p. 34, 1980.

Kadri, I. B., Petroleum Geology of Pakistan, Pakistan Petroleum Limited, Karachi, Pakistan, p. 115-123, 1995.

Kazmi, A. H. and Rana, R. A., Tectonic Map of Pakistan, 1st Edition, Geological Survey of Pakistan, Quetta, Scale 1:2000000, 1982.

Lucia, F. J., Carbonate Reservoir Characterization, An Integrated Approach, Second Edition, Springer, p. 82-84, 2007.

Mohaghegh, S., Balan, B., and Ameri, S., State of the Art in Permeability Determination from Well Log Data, Part 2, Society of Petroleum Engineers, United States of America, Vol. 5, 1995.

Molnar, P. and Tapponnier P., Relation of the Tectonics of Eastern China to the India-Eurasia Collision, Application of Slip-line Field Theory to Large-scale Continental Tectonics, Geology, Vol. 5, p. 212-216, 1977.

O'Brien, D. K., Physical, Acoustic and Electrical Properties of Deep-sea Sediments, Unpublished Ph.D. Thesis, University of Hawaii, Honolulu, 140 p. Hawaii, HI, 1990.

Peters, E. J., Petrophysics, 42 p., 2011.

Purdy, C. C., Enhancement of Long-spaced Sonic Transit Time Data, Society of Petrophysicists and Well Log Analysts 23rd Annual Symposium Transaction, 1982.

Raza, H. A., Ahmed, R., Alam, S., and Ali, S. M., Petroleum Zones of Pakistan, Pakistan Journal of Hydrocarbon Research, Vol. 1, p. 21-56, 1989.

Rider, M. H., the Geological Interpretation of Well Logs, John Wiley and Sons, New York, 1996.

Sadeq, Q. M. and Yusoff, W. I. W. B. W., Carbonate Reservoirs Petrophysical Analysis of Bai Hassan Oil Field North of Iraq, Journal of Bioremediation and Biodegradation, Vol. 6, No. 5, p. 311, 2015.

Salem, H. S., Relationships among Formation Resistivity Factor, Compressional Wave Velocity, and Porosity for Reservoirs Saturated with Multiphase Fluids, Energy Sources, Part A: Recovery, Utilization and Environmental Effects, Vol. 23, No. 7, p. 675-685, 2001.

Salem, H. S. and Chilingarian, G. V., The Cementation Factor of Archie's Equation for Shaly Sandstone Reservoirs, Journal of Petroleum Science and Engineering, Vol. 23, p. 83-93, 1999b.

Schlumberger, Log Interpretation Charts, 2009.

Schlumberger, Log Interpretation Manual/applications, Houston, Schlumberger Well Services, Inc., Vol. II, 1974.

Shah, S. M. I, Stratigraphy of Pakistan, Geological Survey of Pakistan Memoirs 22, 2009.

Shah, S. M. I., Stratigraphy of Pakistan, 138 p., Geological Survey of Pakistan Memoirs 12, 1977.

Sheikh, A. M., Pakistan Energy Yearbook, Hydrocarbon Development Institute of Pakistan, Ministry of Petroleum and Natural Resources, Government of Pakistan, Islamabad, 86 p., 2003.

Siddiqui, N. K., Sui Main Limestone: Regional Geology and the Analysis of Original Pressures of a Closed-system Reservoir in Central Pakistan, Bulletin of American Association of Petroleum Geologists, Vol. 88, No. 7, p. 1007-1035, 2004.

Tabibi, M. and Emadi, M. A., Variable Cementation Factor Determination (Empirical Methods), 13th Middle East Oil Show and Conference in Bahrain, Society of Petroleum Engineers, Conference Paper Number 81485, 2003.

Tainsh, H. R., Stringer, K. V., and Azad, J., Major Gas Fields of West Pakistan, Bulletin of the American Association of Petroleum Geologists, Vol. 43, No. 1, p. 2675-2700, 1959.

Thomas, D. H., Seismic Applications of Sonic Logs, Society of Petrophysicists and Well Log Analysts, Vol. 19, No. 1, p. 1-24, 1978.

Tiab, D. and Donaldson, E. C., Petrophysics, Theory and Practice of Measuring Reservoir Rock and Fluid Transport Properties, 2nd Edition, 243 p. 2004.

Wyllie, M. R. J. and Rose, W. D., Some Theoretical Considerations Related to the Quantitative Evaluation of the Physical Characterization of Reservoir Rock from Electric Log Data, Transactions of American Institute of Mining, Metallurgical and Petroleum Engineers, Vol. 189, p. 105, 1950.